

METHODOLOGY

Open Access



Real-time assessment of relative mitochondrial ATP synthesis response against inhibiting and stimulating substrates (MitoRAISE)

Eun Sol Chang^{1,2}, Kyoung Song³, Ji-Young Song², Minjung Sung², Mi-Sook Lee², Jung Han Oh^{1,2}, Ji-Yeon Kim⁴, Yeon Hee Park⁴, Kyungsoo Jung^{2*} and Yoon-La Choi^{1,2,5*}

Abstract

Background Mitochondria are known to synthesize adenosine triphosphate (ATP) through oxidative phosphorylation. Understanding and accurately measuring mitochondrial ATP synthesis rate can provide insights into the functional status of mitochondria and how it contributes to overall cellular energy homeostasis. Traditional methods only estimate mitochondrial function by measuring ATP levels at a single point in time or through oxygen consumption rates. This study introduced the relative mitochondrial ATP synthesis response against inhibiting and stimulating substrates (MitoRAISE), designed to detect real-time changes in ATP levels as the cells respond to substrates.

Methods The sensitivity and specificity of the MitoRAISE assay were verified under various conditions, including the isolation of mitochondria, variations in cell numbers, cells exhibiting mitochondrial damage, and heterogeneous mixtures. Using peripheral blood mononuclear cells (PBMCs), we analyzed MitoRAISE data from 19 patients with breast cancer and 23 healthy women.

Results The parameters observed in the MitoRAISE data increased depending on the quantity of isolated mitochondria and cell count, whereas it remained unmeasured in mitochondrial-damaged cell lines. Basal ATP, rotenone response, malonate response, and mitochondrial DNA copy numbers were lower in PBMCs from patients with breast cancer than in those from healthy women.

Conclusions The MitoRAISE assay has demonstrated its sensitivity and specificity by measuring relative ATP synthesis rates under various conditions. We propose MitoRAISE assay as a potential tool for monitoring changes in the mitochondrial metabolic status associated with various diseases.

Keywords Relative mitochondrial ATP synthesis rate, Mitochondrial function, ATP, mtDNA copy number, MitoRAISE

*Correspondence:

Kyungsoo Jung
ksjung0820@skku.edu
Yoon-La Choi
ylachoi@skku.edu

Full list of author information is available at the end of the article



© The Author(s) 2024. **Open Access** This article is licensed under a Creative Commons Attribution-NonCommercial-NoDerivatives 4.0 International License, which permits any non-commercial use, sharing, distribution and reproduction in any medium or format, as long as you give appropriate credit to the original author(s) and the source, provide a link to the Creative Commons licence, and indicate if you modified the licensed material. You do not have permission under this licence to share adapted material derived from this article or parts of it. The images or other third party material in this article are included in the article's Creative Commons licence, unless indicated otherwise in a credit line to the material. If material is not included in the article's Creative Commons licence and your intended use is not permitted by statutory regulation or exceeds the permitted use, you will need to obtain permission directly from the copyright holder. To view a copy of this licence, visit <http://creativecommons.org/licenses/by-nc-nd/4.0/>.

Background

Mitochondria control biological processes that occur in almost all cells of the human body, such as synthesis of iron-sulfur clusters, apoptosis, cell signaling, maintenance of calcium homeostasis, and maintenance of reactive oxygen species levels [1]. The classic role of mitochondria is oxidative phosphorylation (OXPHOS), a metabolic pathway that produces ATP by utilizing the energy released during nutrient oxidation [2]. The first OXPHOS pathway involves complexes I, III, and IV using electrons from NADH, whereas the second pathway involves complexes II, III, and IV using FADH₂ [3]. The continuous pumping of protons increases the hydrogen ion concentration and reduces pH, eventually generating a membrane potential. This membrane potential is utilized by complex V (ATP synthase) to produce ATP [4–6].

Although the OXPHOS pathway is a major source of ATP in cells, its function in cancer has been overlooked because it was previously presumed that cancer cells predominantly utilize aerobic glycolysis as their main energy synthesis process [7]. Accordingly, multiple studies have shown a correlation between reduced OXPHOS activity and cancer malignancies [8]. However, there are also numerous contradictory studies demonstrating that cancers rely heavily on OXPHOS and that there is heterogeneity in cellular metabolism [9–11]. The mitochondrial ATP synthesis rate through the OXPHOS system can no longer be overlooked, even in cancer, because it is representative of mitochondrial metabolism. The correlation between oxygen consumption and mitochondrial metabolism is well established. In this regard, the oxygen consumption rate (OCR) assay is one of the most widely used methods for real-time measurement mitochondrial metabolic status [12]. Another assay for real-time measurement simultaneously analyzes ATP production and oxygen consumption using a device that combines respirometry with fluorescence signal detection. The ATP/O ratio analyzed by this assay indicates the efficiency of the cellular respiratory process [13, 14].

In this study, we designed a new technique called the relative mitochondrial ATP synthesis response against inhibiting and stimulating substrates (MitoRAISE) assay to measure the relative rate of ATP synthesis and investigated its potential clinical usefulness. First, we validated the MitoRAISE assay under various conditions using isolated mitochondria and cell lines. Subsequently, we explored the clinical significance of the MitoRAISE results in clinical samples.

Methods

Reagents

The mitochondrial assay solution (MAS) buffer was prepared according to the manufacturer's protocol (Agilent Technologies, Santa Clara, CA, USA) using 220 mM mannitol, 70 mM sucrose, 10 mM KH₂PO₄, 5 mM MgCl₂, 2 mM HEPES, 1 mM ethylene glycol tetraacetic acid, and 0.2% bovine serum albumin (BSA) (pH 7.4). The plasma membrane permeabilizer (PMP) was purchased from Agilent Technologies (Santa Clara, CA, USA). P¹, P⁵-Di (adenosine-5') pentaphosphate pentasodium salt (Ap5A; D4022), ADP, L-glutamic acid, L(-) malic acid, sodium succinate dibasic hexahydrate (succinate), rotenone, and sodium malonate dibasic (malonate) were purchased from Sigma-Aldrich (St. Louis, MO., USA). 2-(2-(3-Chlorophenyl)hydrazinylydene)propanedinitrile (CCCP) and Carbonyl cyanide 4-(trifluoromethoxy) phenylhydrazone (FCCP) were purchased from Abcam (Abcam, Cambridge, MA, USA).

Cell lines

All the cell lines used in this study were purchased from either the American Type Culture Collection (Manassas, VA, USA) or the Korean Cell Line Bank (Seoul, Korea). A549-Rho-0 cells were purchased from Kerfast, Inc. (Boston, MA, USA). Multiple breast cancer cell lines: BT-20, BT-474, BT-549, HCC1428, MCF7, MDA-MB-231, ZR-75-1, from mammary glands were tested as well as HeLa cell line from the uterus, and BEAS-2B and A549 cell lines from the lung. All cells tested negative for mycoplasma, and cell lineages were confirmed using short tandem repeat analysis.

MitoRAISE assay

Samples were prepared in mitochondrial assay solution (MAS; 220 mM mannitol, 70 mM sucrose, 10 mM KH₂PO₄, 5 mM MgCl₂, 2 mM HEPES, 1 mM EGTA, and 0.2% fatty acid-free BSA, pH 7.4). The XF plasma membrane permeabilizer (PMP) was purchased from Agilent Technologies (Santa Clara, CA, USA). P¹, P⁵-Di (adenosine-5') pentaphosphate pentasodium salt (Ap5A; D4022), ADP, L-glutamic acid, L(-) malic acid, sodium succinate dibasic hexahydrate (succinate), rotenone, and sodium malonate dibasic (malonate) were purchased from Sigma-Aldrich (St. Louis, MO., USA). 2-(2-(3-Chlorophenyl)hydrazinylydene)propanedinitrile (CCCP) and carbonyl cyanide 4-(trifluoromethoxy) phenylhydrazone (FCCP) were purchased from Abcam (Abcam, Cambridge, MA, USA). The MitoRAISE method is described in detail in Sect. 3.1.

Mitochondrial isolation

Mitochondria were isolated as previously described [15]. Briefly, cells were harvested from culture dishes in 5 mL homogenizing buffer. A 200- μ L solution of subtilisin A (4 mg/mL) was added to the buffer, and the solution was drawn into a 22G syringe 20 times on ice. The homogenized solution was then centrifuged at $9,000\times g$ for 10 min at 4 °C. The pellet was collected in 500 μ L of ice-cold respiration buffer and quantified using the Pierce BCA protein assay kit (Thermo Fisher Scientific, Waltham, MA, USA).

PBMC isolation

Nineteen patients with breast cancer and twenty-three healthy women were recruited at the Samsung Medical Center (SMC), Seoul, South Korea, between October 2021 and November 2022. Whole blood (10 mL) was extracted after obtaining informed consent from the participants with the approval of the SMC Institutional Review Board (IRB No. SMC 2019–08-119, SMC 2021–08-063). All blood samples were subjected to Ficoll-Paque Plus (Cytivia, Marlborough, MA, USA) gradient-based PBMC isolation within two hours of sample collection. The resulting PBMC pellet was washed again with eBioscience 1X RBC lysis buffer (Invitrogen, Waltham, MA, USA), according to the manufacturer's protocol. The cell pellet was resuspended in MAS buffer after removal of the supernatant.

Cellular plasma membrane permeabilization

Cells or peripheral blood mononuclear cells (PBMCs) were treated with 5–10 nM XF PMP (Agilent Technologies, Santa Clara, CA, USA) and incubated at room temperature for 10 min. Membrane permeabilization was measured as the percentage of trypan blue-stained cells, using a Countess automated cell counter (Thermo Fisher Scientific, Waltham, MA, USA). Further experiments were performed only when more than 90% of PMP-permeabilized cells were stained. PMP cytotoxicity was measured using an EZ-Cytox assay (DoGenBio, Seoul, South Korea).

Total ATP level measurement

Total ATP was measured using the ATPlite Luminescence ATP Assay System (PerkinElmer, Waltham, MA, USA), following the manufacturer's protocol. Briefly, standard ATP and samples were seeded into a 96-well white plate, and up to 50 μ L of lysis solution was added, followed by shaking for 2 min. Subsequently, 50 μ L of ATPlite solution was added and shaken for 10 min in the dark. ATP level was measured using a Mithras LB 943 Monochromator Multimode Reader (Berthold Technologies GmbH and Co., Wildbad, Germany).

Mitochondrial DNA copy number

The mitochondrial DNA copy number (mtDNA-CN) was determined using real-time quantitative polymerase chain reaction (qPCR) on the PRISM[®] 7900HT Fast Real-Time PCR System (Applied Biosystems, Foster City, CA, USA). Primer sequences (Cosmo Genetech, Daejeon, South Korea) are listed in Supplementary Table 1. The mtDNA-CN was calculated by adjusting the standard curve of a plasmid calibrator that contained exactly one copy of mtDNA and one copy of nuclear DNA.

Validation of A549-Rho-0 cells

To validate the missing mtDNA in A549-Rho-0 cells, we tested a total of 1000 ng of RNA from the cell lines to synthesize the cDNA and tested designed primers for mitochondrially encoded NADH dehydrogenase 1 (mtND1) gene on 1% agarose (Affymetrix, Santa Clara, CA, USA) gel. The designed primers are shown in Supplementary Table 2.

Imaging of mitochondrial membrane potential

5×10^4 cells were seeded in a 6-well plate and grown for two days. FCCP and CCCP was treated and after 30 min incubation, 50 nM of MitoTracker Red CMXRos (ThermoFisher Scientific, Waltham, MA, USA) was treated for 10 min. After washing, cells were observed under a fluorescence microscopy (10X, 1.5X crop). Images from the fluorescence microscope was then analyzed with ImageJ (National Institutes of Health, Bethesda, MD, USA).

Statistical analysis

The unpaired Student's *t*-test was used to evaluate differences between groups. Pearson's correlation analysis was used to investigate the association between clinical information and experimental data. Data are shown as the mean values \pm SD of at least three independent experiments. All statistical experiments were two-sided, and *p*-values < 0.05 were considered statistically significant. GraphPad Prism software (version 9.5.1; San Diego, CA, USA) was used for all statistical analyses. Data were processed and figures were generated using RStudio (<https://www.rstudio.com>), Microsoft Excel, and GraphPad Prism.

Results

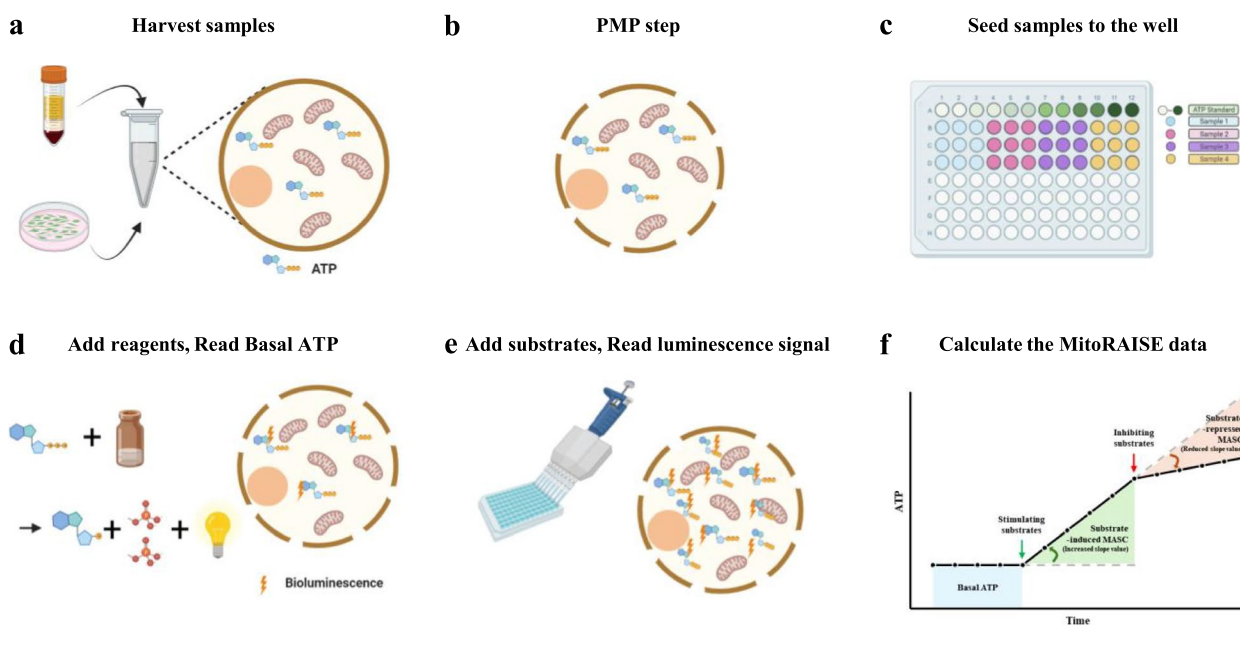
Development of MitoRAISE and its workflow

The MitoRAISE assay was designed to measure real-time relative ATP synthesis rate (ASR) in response to substrate stimulation and inhibition. To investigate ASR, we first prepared PMP-permeabilized cells using 5–10 nM XF PMP. PMP causes less damage to both the cell and mitochondrial membranes than detergent-based reagents such as digitonin or saponin [16]. Since trypan blue

passes through both PMP-permeabilized and dead cells, the cells were stained to quantify the labeled cells before and after permeabilization. The MitoRAISE assay was performed when fewer than 10% of the labeled cells were observed before permeabilization, and more than 90% of the labeled cells were observed after permeabilization.

PMP-permeabilized cells were seeded in a 96-well white plate, and MAS containing the adenylate kinase inhibitor, Ap5A (final concentration: 200 μM), was added up to 50 μL, and the mixture was shaken for 2 min in the dark. Subsequently, 50 μL of the ATPlite solution with 100 μM ADP was added, and the mixture was again shaken for 2 min in the dark. After a 10-min incubation, luminescence was measured at 2-min intervals over a 10-min period. Before each of the five measurements, the plate was shaken for 5 s. The average value of the luminescence signals represented the amount of ATP, which was referred to as Basal ATP.

Next, 10 μL of stimulating substrates were added, and luminescence was measured every 2- min over a 10-min period, with the plate being shaken for 5 s before each measurement. The rate of increase in luminescence signals represents the relative ATP synthesis rate induced by the stimulating substrates, referred to as stimulating substrate-induced ASR. Finally, 10 μL of inhibiting substrates were added, and luminescence was measured every 2-min over a 10-min period, with the plate being shaken for 5 s before each measurement. The rate of decrease in the luminescence signal, compared to ASR induced by stimulating substrates, represents the relative ATP synthesis rate inhibited by substrates, referred to as the inhibiting substrate-repressed ASR. All luminescence signals were calibrated to the ATP levels at each time point against real-time quantitative ATP standard curves using ATP standard solutions (Fig. 1).



Parameter values	Equation
Basal ATP	Average ATP levels before first injection
Substrate-induced ASR	Average slope measurement after stimulating substrate injection
Substrate-repressed ASR	(Substrate-induced ASR) - (Average slope measurement after inhibiting substrate injection)
Inhibiting substrate Response	(Substrate-repressed ASR) / (Substrate-induced ASR)

Fig. 1 Workflow of the MitoRAISE assay. **a** Cells and peripheral blood mononuclear cells (PMBCs) were harvested from a culture plate or isolated from whole blood samples, respectively. **b** Cells were treated with XF Plasma Membrane Permeabilizer (PMP). **c** PMP-permeabilized cells were seeded in a 96-well white plate. **d** Mitochondrial assay solution (MAS) buffer with Ap5A and ADP was added to the wells, followed by the addition of ATPlite solution. The luminescence is then measured. **e** Stimulating substrates are added to induce the ATP synthesis reaction. Then, the luminescence was measured. This was followed by the addition of inhibiting substrates to repress the ATP synthesis reaction, after which the luminescence was measured again. **f** The luminescence was calibrated to ATP levels and then the MitoRAISE data, such as basal ATP, substrate-induced ASR, and substrate-repressed ASR, were calculated

Validation of MitoRAISE using isolated mitochondria and viable cells

To validate the sensitivity and specificity of the MitoRAISE assay, we used mitochondria isolated from A549 cells via dissociation and differential filtration as previously described [15]. Quantification of the isolated mitochondria was performed using a BCA protein assay. Depending on the amount of isolated mitochondria, there was an increase observed in both glutamic acid with malic acid (GM)-induced ASR (21.71 nM/min, 51.24 nM/min, 107.06 nM/min), associated with mitochondrial complex I, and succinate (S)-induced ASR (37.25 nM/min, 91.89 nM/min, 210.60 nM/min), associated with mitochondrial complex II. The addition of the inhibiting substrates rotenone (Rot) and malonate (Mal) resulted in a reduction of approximately 90% in the ASR induced by GM and S, representing Rot- and Mal-repressed ASR (Fig. 2a and Supplementary Fig. 1a). No change in ASR was observed when distilled water was used instead of the substrate (Supplementary Fig. 2a). To determine whether ASR reading corresponded to a false-positive signal resulting from nonspecific interference by materials, we conducted the MitoRAISE assay using a blank sample consisting of MAS buffer only. No non-specific interference was observed at the appropriate

concentrations of the material used in the experiment (Supplementary Fig. 2c). These results indicate that ASR values are derived from mitochondrial ATP synthesis.

We further validated the results of the MitoRAISE assay at the cellular level. To measure ASR in living cells, the permeabilization process is crucial to allow the substrates to enter and react within the cells. A549 cells were treated with the XF PMP at concentrations ranging from 0 to 10 nM. PMP (5 nM) was sufficient to fully permeabilize the membranes of A549 cells (Supplementary Fig. 3a). Compared with the ASR of A549 cells treated with 5 nM PMP, A549 cells that did not undergo complete permeabilization with 2 nM PMP exhibited a lower ASR. Conversely, in A549 cells treated with 10 nM PMP, ASR values were similar (Supplementary Fig. 3b and c). No change in ASR was observed when distilled water was used instead of the substrate (Supplementary Fig. 2b). These data suggest that PMP does not affect the mitochondrial membrane and that the MitoRAISE assay is capable of measuring ASR at the cellular level.

To evaluate the sensitivity and specificity of the MitoRAISE assay at the cellular level, we analyzed ASR under various conditions, including varying cell numbers, cells with mitochondrial damage, and heterogeneous mixtures. Initially, we measured ASR using varying numbers

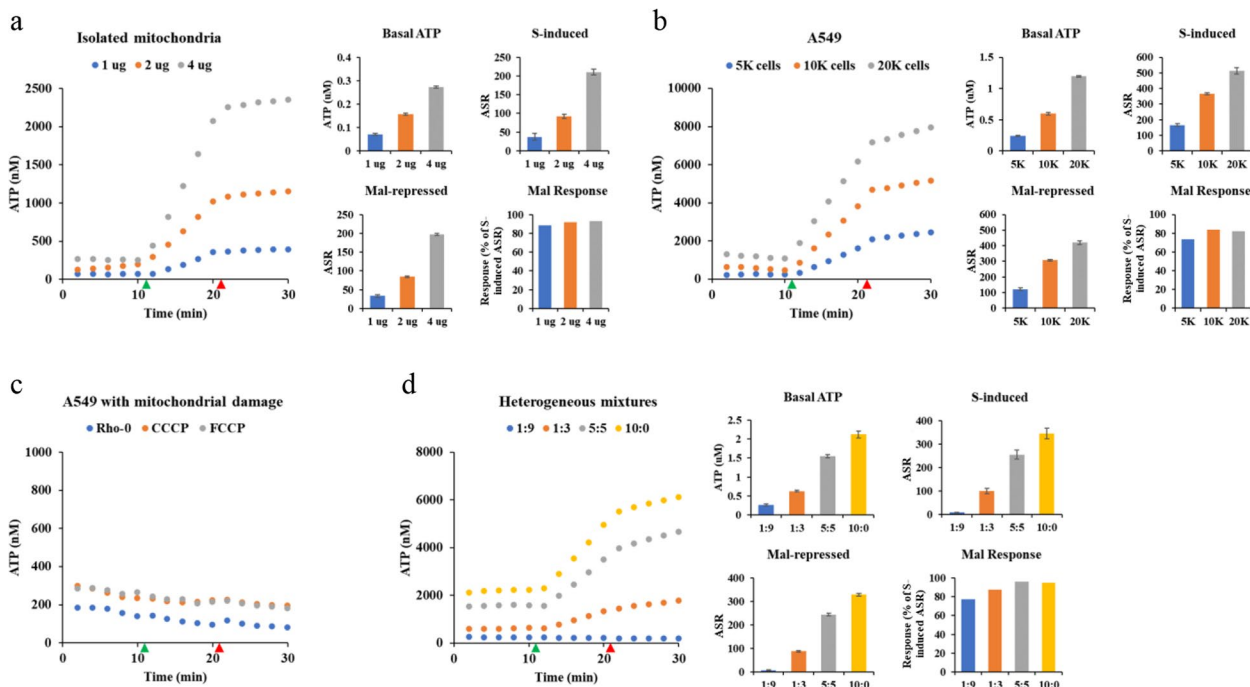


Fig. 2 Validation of the MitoRAISE assay using isolated mitochondria and viable cells. Dot plots of the real-time accumulation of ATP level from (a) isolated mitochondria, (b) varying cell numbers, (c) cells with mitochondrial damage, and (d) heterogeneous mixtures. Bar graphs of the basal ATP levels, the change in the slope of relative ATP synthesis rate after succinate injection (S-induced), the change in the slope of relative ATP synthesis rate after malonate injection (Mal-repressed), and the mal-repressed of S-induced ratio (Mal Response). The green triangle indicates the time at which succinate was injected, while the red triangle indicates the time at which malonate was injected

of A549 cells. The parameters of the MitoRAISE assay, such as Basal ATP, and S- and GM-induced ASR, exhibited an increase corresponding to the cell number (Fig. 2b and Supplementary Fig. 1b). Additionally, the MitoRAISE assay was validated using mtDNA-depleted A549 cells (A549-Rho-0). Gel electrophoresis showed that A549-Rho-0 cells lacked mitochondrial DNA (Supplementary Fig. 4a). Furthermore, A549 cells treated with CCCP or FCCP were confirmed to have damaged mitochondrial membrane potentials using MitoTracker Red CMXRos staining (Supplementary Fig. 4b). No response to the activation or inhibition of substrates was observed in A549 cells with mitochondrial damage (Fig. 2c and Supplementary Fig. 1c). To further evaluate the specificity of MitoRAISE assay, we prepared heterogeneous mixtures of PMP-permeabilized and intact cells at ratios of 1:9, 1:3, 5:5, and 10:0 (Supplementary Fig. 1e). As the proportion of PMP-permeabilized cells in the mixture increased, the ASR induced by GM and S also showed a corresponding increase (Fig. 2d and Supplementary Fig. 1d). Overall, these results indicate that the MitoRAISE assay demonstrates sensitivity and specificity for PMP-permeabilized cells with intact mitochondria, enabling real-time measurement of relative mitochondrial ATP synthesis rate.

A comprehensive analysis of mitochondria in cell lines using MitoRAISE

To assess the potential utility of the MitoRAISE assay results, we conducted a comprehensive analysis of the Total ATP level, ASR, and mtDNA copy number (mtDNA-CN) in seven breast cancer cell lines and three additional cell lines. Total ATP levels were determined using a conventional luminescence-based ATP detection assay requiring cell lysis. mtDNA-CN was determined using PCR-based assays. The data, including Total ATP levels and ASR, exhibited variance within the cell lines (Supplementary Fig. 5). This variance may be caused by batch effects or other factors, such as changes in ATP synthesis regulated during cell cycle progression [17]. To determine whether this variance was the result of different batches or changes in cell metabolism, we performed a correlation analysis within each cell line. Some cell lines (e.g., MCF7, BT-474, BT-549, A549, and BEAS-2B) showed a positive correlation between Total ATP level and both GM-induced and S-induced ASR (Fig. 3a). MDA-MB-231, ZR-75-1, HeLa, BT-20, and HCC1428 cells showed a negative or no correlation between Total ATP level and GM-induced and S-induced ASR (Fig. 3b). Previous studies have indicated that MCF7 and BT-474 cells demonstrate metabolic profiles characterized by relatively high mitochondrial respiration and low glycolysis, whereas MDA-MB-231 and BT-20 cells exhibit metabolic profiles characterized by high glycolysis and low

mitochondrial respiration [18]. These data suggest that the observed variances are likely to be influenced more by the cellular metabolism status than by batch effects.

Based on the correlation analysis, the cell lines were divided into two groups: one exhibiting a positive correlation between Total ATP levels and substrate-induced ASR (PC group) and the other showing no positive correlation (NC group). MCF7, BT-474, BT-549, A549, and BEAS-2B cells comprise the PC group, whereas MDA-MB-231, ZR-75-1, HeLa, BT-20, and HCC1428 cells constitute the NC group. We performed an unpaired *t*-test to investigate the differences between these groups. No statistically significant differences were observed between the groups (Supplementary Fig. 6). Therefore, we performed a correlation analysis using Pearson's correlation coefficient for each group. Notably, a statistically significant positive correlation was observed between Total ATP levels and Basal ATP as well as mtDNA-CN in the PC group (Fig. 3c and Supplementary Fig. 7a) but not in the NC group (Fig. 3d and Supplementary Fig. 7b). Although no statistically significant correlation was found between Total ATP, Basal ATP, GM- and S-induced ASR, there appeared to be a tendency toward a positive correlation only in the PC group (Fig. 3c and Supplementary Fig. 7a), whereas a trend toward a negative correlation appeared to be present in the NC group (Fig. 3d and Supplementary Fig. 7b). These data suggest that the PC group is more likely to be dependent on OXPHOS for ATP production. In summary, we propose the possibility that the MitoRAISE assay could potentially predict the cellular metabolic type of the sample.

Assessing the clinical relevance of relative mitochondrial ATP synthesis rate

To investigate the clinical significance of the MitoRAISE results, PBMCs were collected from 23 healthy women and 19 patients with breast cancer. Subsequently, the Total ATP, Basal ATP, GM- and S-induced ASR, Rot- and Mal-repressed ASR, and mtDNA-CN levels were measured (Table 1). No statistically significant differences were noted in height, weight, or BMI between healthy individuals and patients with breast cancer, except for age ($P < 0.0001$) (Fig. 4a and Supplementary Fig. 8a). Patients with breast cancer appeared to have lower Basal ATP levels compared to healthy individuals, though their Total ATP levels did not seem to be lower. Although no difference was noted in S-induced ASR between the groups, GM-induced ASR and the ratio of GM-induced ASR to S-induced ASR were significantly higher in patients with breast cancer ($P = 0.0096$ and $P = 0.0184$, respectively). Additionally, mtDNA-CN and the response to the inhibitors rotenone and malonate were lower in patients with breast

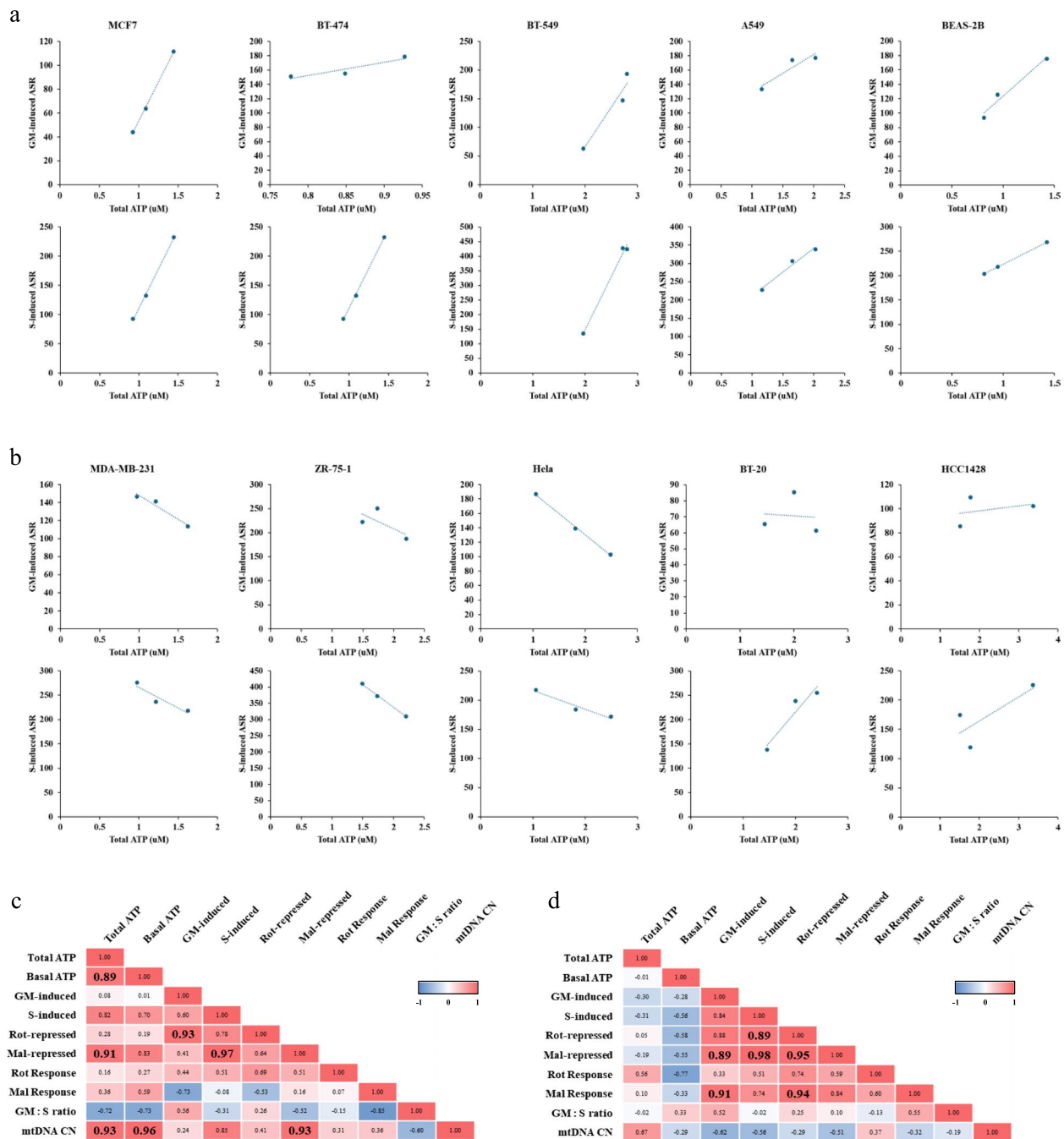


Fig. 3 A comprehensive analysis of mitochondria in cell lines using the MitoRAISE assay. **a** Dot plots of cell lines show a positive correlation between total ATP levels and (upper) glutamic acid and malic acid (GM)-induced ASR, and (lower) succinate (S)-induced ASR. **b** Dot plots of cell lines show a negative or no correlation between total ATP levels and (upper) glutamic acid and malic acid (GM)-induced ASR, and (lower) succinate (S)-induced ASR. Pearson correlation analysis table of **(c)** the PC group and **(d)** the NC group. The PC group is defined as the group in which a positive correlation exists between Total ATP levels and both GM- and S-induced ASRs in the cell line. The NC group is defined as the group in which a negative or no correlation exists between Total ATP levels and both GM- and S-induced ASRs in the cell line

cancer ($P=0.0002$, $P=0.0030$, and $P=0.0147$, respectively) (Fig. 4a and Supplementary Fig. 8a). These data indicate that the mitochondrial metabolic status of

PBMCs differs between healthy women and patients with breast cancer. Mitochondria are also associated with aging [19]. Unfortunately, our data revealed

Table 1 Clinical characteristics of the study participants

	Healthy women		Patients with breast cancer	
	Mean	(Range)	Mean	(Range)
Age (years)	37.2	(24–67)	53.1	(34–68)
Height (cm)	161.6	(150.4–170.5)	158.8	(146.1–172.0)
Weight (kg)	58.1	(41.1–79.9)	60.2	(44.2–75.8)
BMI	22.3	(18.2–32.0)	23.9	(16.7–31.0)
Total ATP	1.1	(0.8–1.6)	1.2	(0.9–2.0)
Basal ATP	1.0	(0.6–2.0)	0.5	(0.2–1.3)
GM-induced	36.6	(18.2–71.4)	48.6	(20.3–71.8)
S-induced	125.4	(63.3–188.1)	135.6	(90.7–216.4)
Rot-repressed	24.8	(8.7–50.7)	25.4	(4.7–41.7)
Mal-repressed	100.9	(36.8–170.0)	94.7	(35.6–184.6)
Rot Response	67.6	(26.5–89.1)	52.1	(18.5–69.2)
Mal Response	78.5	(58.1–94.9)	67.8	(39.3–86.8)
GM: S ratio	0.3	(0.2–0.4)	0.4	(0.2–0.6)
mtDNA CN	99.1	(45.1–158.1)	64.2	(19.3–123.2)

age-related differences between healthy individuals and patients with breast cancer. To investigate whether the differences in the mitochondrial metabolic status of PBMCs between healthy individuals and patients with breast cancer were age-related, we conducted a correlation analysis using all samples. Basal ATP, rotenone response, malonate response, and mtDNA-CN levels were negatively correlated with age (Supplementary Fig. 8b and 9a). These results suggest that differences in the mitochondrial metabolic status of PBMCs may be age-related or differ between patients with breast cancer and healthy women. Further research is needed to identify these differences by recruiting individuals from various age groups.

To further investigate the difference in the clinical significance of the mitochondrial metabolic status between PBMCs from healthy individuals and those from patients with breast cancer, we conducted a correlation analysis using Pearson's correlation coefficient for each group. In the healthy individuals group, mtDNA-CN showed a negative correlation with age and BMI scores, and a positive correlation with GM- and S-induced ASR. No correlation was observed between mtDNA-CN and the other variables in patients with breast cancer. Notably, a positive correlation was observed between Basal ATP levels and GM- and S-induced ASR in the healthy individual group, but no correlation was observed in the breast cancer patient group (Fig. 4b and c, and Supplementary Fig. 9b and c). These results were similar to those of the comparison between the PC and NC groups in the cell line experiments (Fig. 3c and d). Overall, our findings suggest that

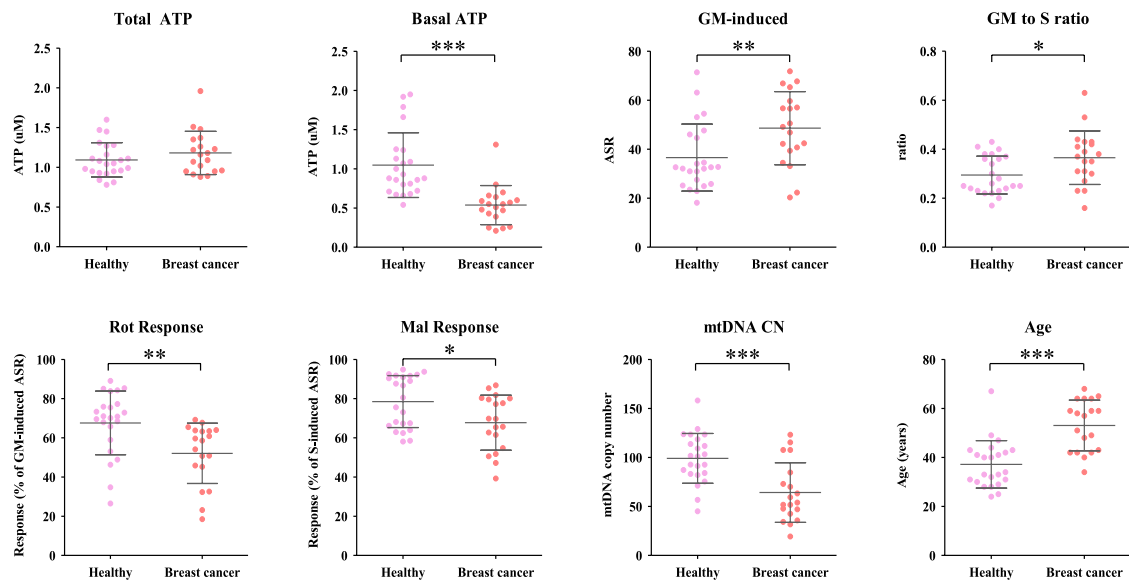
MitoRAISE analysis has the potential to be utilized for detecting the mitochondrial metabolic status.

Discussion

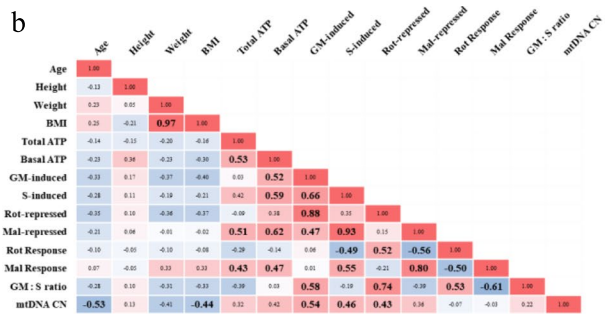
Since the discovery of ATP in 1929 and its function as an energy carrier in the late 1930s, the importance of ATP synthesis via OXPHOS has never been questioned [20, 21]. Among the co-working protein complexes in the mitochondria, mitochondrial complex I is the largest, and its dysfunction is known to be directly linked to mitochondrial malfunction in multiple diseases, such as dementia and cancer [22, 23]. Mitochondrial complex II, in contrast, is the smallest protein complex involved in both the tricarboxylic acid cycle and OXPHOS. Complications in complex II can also lead to cancer, cell death, and necrosis [24, 25]. Although mitochondrial complexes I and II differ in their roles within the electron transport chain, as well as in the occurrence of diseases resulting from dysfunction in each complex, mitochondrial functional studies utilize analyses of total ATP level or indirect measurement data, such as oxygen consumption and mitochondrial complex enzyme activity [26, 27].

The traditional ATP assay and the oxygen consumption rate (OCR) assay are distinct methods, each characterized by unique features and available conditions. Traditional ATP assays quantify ATP using the enzyme luciferase, which reacts with ATP to emit light. However, this process destroys cells, preventing the observation of changes over time within a cell. Nonetheless, this assay offers the advantage of assessing the energy level, such as ATP level, and is relatively simple and fast to analyze. The OCR assay, on the other hand, evaluates metabolic activity by measuring the amount of oxygen consumed by the cell. An advantage of the OCR assay is the ability to analyze live cells, facilitating the observation of changes over time. However, the OCR assay is an indirect measure of mitochondrial metabolism because oxygen consumption is a byproduct of the electron acceptor in the OXPHOS pathway during ATP production. Additionally, this method requires relatively expensive equipment and may involve complexity in data interpretation. The MitoRAISE assay has been modified from the traditional ATP assay to overcome its limitations while leveraging the benefits of the OCR assay. The MitoRAISE assay can measure relative ATP synthesis rate by serially measuring substrate-induced changes in ATP level in living cells. Although the MitoRAISE assay cannot be conducted in intact cells and is exclusively performed in PMP-permeabilized cells, the intactness of mitochondria enables measurement of changes in ATP level in response to the reagent. For more accurate measurement of changes in ATP level, a luminometer with a programmable injector,

a



b



c

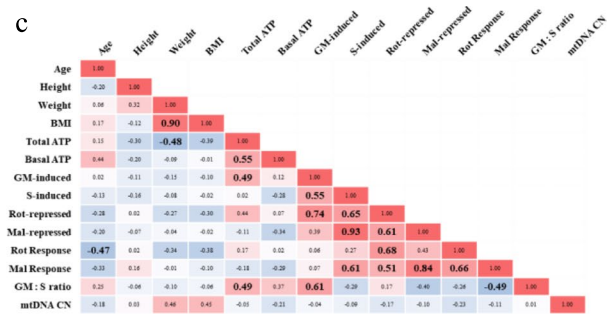


Fig. 4 Assessing the clinical relevance of *r* ATP synthesis rate. **a** Scatter dot plot of MitoRAISE data comparing healthy participants with patients with breast cancer. Pearson correlation analysis table of **(b)** healthy women and **(c)** patients with breast cancer. *p*-values are denoted as follows: * for *P* < 0.05, ** for *P* < 0.01, and *** for *P* < 0.001

repeat measurement capability, and shaking options is required.

Fluorescence-based approaches and MitoRAISE assay share similarities in measuring products of reactions involving ATP, enzymes, and substrates. In the fluorescence-based approach, ATP produced by mitochondria is consumed to convert glucose to glucose-6-phosphate, which is then converted to 6-phosphogluconolactone by glucose-6-phosphate dehydrogenase (G6PD). During this process, NADPH, which exhibits autofluorescence, accumulates in proportion to ATP consumption. The rate of ATP production can be quantified by monitoring the fluorescence intensity that increases over time [13]. Another fluorescence-based approach measures changes in the fluorescence intensity of Magnesium Green (MgGr), which fluoresces when bound to Mg²⁺, based on the different dissociation constants of ADP and ATP for Mg²⁺ [14]. Fluorescence-based approaches have the advantage

of being able to simultaneously measure respiratory consumption, but equipment capable of simultaneously measuring respiratory consumption and fluorescence is required. In MitoRAISE assay, ATP generated in the mitochondria catalyzes the luciferin and luciferase reaction, releasing oxyluciferin, CO₂, AMP, and light. The intensity of emitted light directly correlates with ATP concentration. Unlike traditional ATP assays that measure total ATP level after cell lysis, MitoRAISE assay uses permeabilized cells with intact mitochondria, enabling real-time measurement of accumulated ATP level. The relative rate of ATP synthesis can be easily quantified by monitoring the increasing intensity of emitted light over time in a readily available luminometer.

The MitoRAISE assay uses a nontoxic permeabilization agent to deliver substrates directly to the mitochondria within cells [28]. PMP (5 nM) was sufficient to fully permeabilize the cells, and higher concentrations of PMP

did not harm the cells in terms of ATP synthesis rate (Supplementary Fig. 3). Other plasma membrane permeabilizers such as saponin and digitonin exhibited cell toxicity even at low concentrations, whereas PMP did not show cytotoxicity (Supplementary Fig. 10). The MitoRAISE assay can provide more informative insights into the current status of mitochondria. It not only quantifies the amount of ATP (Basal ATP) but also demonstrates changes in ATP levels when mitochondria are stimulated by substrates (substrate-induced ASR) and the response to inhibitory substrates (substrate-repressed ASR). A slight difference was noted between the Total ATP level measured using the conventional ATP detection kit and the Basal ATP level measured using the MitoRAISE assay. Conventional ATP detection kits measure ATP levels extracted by cell lysis, which may include nuclear, cytosolic, and mitochondrial ATP. In contrast, the MitoRAISE assay measures the ATP levels in cells after permeabilization, primarily by capturing cytosolic ATP. Until now, it was unknown whether luciferin was transported to the nucleus and mitochondria.

The phosphate to oxygen ratio (P/O ratio) is a critical metric in bioenergetics that measures the efficiency of oxidative phosphorylation in mitochondria. It represents the number of ATP molecules synthesized per atom of oxygen reduced, a pivotal ratio for understanding how effectively mitochondria convert substrates into ATP [29]. *In vivo* mouse studies have shown that the P/O ratio decreases with age and that reactive oxygen species exacerbate this decrease. This decrease is more pronounced in older mice, and research suggests that it is associated with a reduction in mitochondrial ATPase activity [30]. However, there are reports indicating that the P/O ratio is not a reliable indicator of mitochondrial function in cancer, as the metabolic nature of cancer allows ATP to be synthesized via alternative pathways [31]. Despite the controversy regarding the association between disease and changes in the P/O ratio, it remains an accurate indicator of oxidative phosphorylation efficiency. MitoRAISE assay provides a relative rate of ATP synthesis by measuring the changing level of ATP in response to a substrate. To find the absolute rate of ATP synthesis, it is necessary to measure the rate of oxygen consumption to ensure that the correct P/O ratio is produced.

The MitoRAISE assay offers the advantage of utilizing cell suspensions, such as PBMCs. PBMCs are readily available sources of patient samples and are currently receiving attention for their potential use as predictive biomarkers for multiple diseases [32]. Several studies have shown the use of PBMCs as potential tools to determine the inflammatory and metabolic status in various disease states, including chronic fatigue syndrome and type 2 diabetes [33, 34].

The findings of this study indicate that PBMCs from patients with breast cancer show lower Basal ATP, rotenone response, malonate response, and mtDNA copy numbers than PBMCs from healthy individuals (Fig. 4a). As mitochondria are known to be associated with the aging process, we carried out a correlation analysis using a mixed sample of healthy individuals and patients with breast cancer. The analysis revealed a negative correlation between age and Basal ATP levels, rotenone response, malonate response, and mtDNA copy number (Supplementary Fig. 7b). Regrettably, patients with breast cancer were older than the healthy participants (Fig. 4a). Therefore, further research is needed to confirm whether these differences are attributable to age or disease.

The major limitation of this study is that further validation is needed to confirm it yields an accurate P/O ratio to ensure the MitoRAISE data accurately represents the absolute rate of ATP synthesis. Additionally, the cells were not synchronized when conducting correlation analyses between total ATP levels and ASR induced by GM and S using cell lines. More detailed studies are required to investigate mitochondrial metabolism according to the cell cycle accurately. Furthermore, the relationship between aging and mitochondrial metabolism is intimate. However, the assessment of the clinical relevance of mitochondrial metabolism status lacked consideration of age disparities among groups. Future investigations will address this gap by recruiting young breast cancer patients or older healthy participants, facilitating a more precise examination of the variations in clinical significance associated with mitochondrial metabolic status. Despite these limitations in the utilization of the MitoRAISE assay, our data demonstrate that MitoRAISE analysis can sensitively and specifically measure the relative ATP synthesis rate.

Conclusions

In this study, we demonstrated the feasibility of using the MitoRAISE assay as a method in mitochondrial research for the real-time measurement of relative mitochondrial ATP synthesis rate. Additionally, these findings suggest that MitoRAISE analysis has the potential to be utilized for monitoring changes in the mitochondrial metabolic status related to various diseases, such as aging, cancer, chronic fatigue syndrome, and type 2 diabetes.

Abbreviations

ATP	Adenosine triphosphate
ADP	Adenosine diphosphate
Ap5A	P ¹ , P ⁵ -di (adenosine-5') pentaphosphate pentasodium salt
CCCP	2-(2-(3-Chlorophenyl)hydrazinylidene)propanedinitrile
DNA	Deoxyribonucleic acid
OXPHOS	Oxidative phosphorylation
PMP	Plasma membrane permeabilizer
PBMC	Peripheral blood mononuclear cells
GM	Glutamic acid and malic acid

S	Succinate
Rot	Rotenone
Mal	Malonate
NADH	Nicotinamide adenine dinucleotide
FADH ₂	Flavin adenine dinucleotide
FCCP	Carbonyl cyanide 4-(trifluoromethoxy) phenylhydrazine

Supplementary Information

The online version contains supplementary material available at <https://doi.org/10.1186/s40170-024-00353-3>.

Supplementary Material 1.

Acknowledgments

Figures were created using BioRender.com.

Authors' contributions

E.S.C.: Investigation, data curation, methodology, visualization, writing the original draft, writing the review, and editing. K.S.: Writing, reviewing, and critical editing. J.Y.S.: Critical comments on the manuscript. M.J.S.: Sample preparation, M.S.L.: Critical comments on the manuscript, J. H. O.: investigation and validation. J.Y.K.: Sample preparation. Y.H.P.: Sample preparation; K.S.J.: Conceptualization, data curation, supervision, and writing the review. Y.L.C. conceptualized, supervised, and wrote the reviews.

Funding

This research was supported by a National Research Foundation of Korea (NRF) grant funded by the Korean government (2022R1C1C2012725 and RS-2023-00217189), and a grant from the Korea Health Technology R&D Project through the Korea Health Industry Development Institute (KHIDI), funded by the Ministry of Health and Welfare, Republic of Korea (HR22C136301).

Availability of data and materials

No datasets were generated or analysed during the current study.

Declarations

Ethics approval and consent to participate

Nineteen patients with breast cancer and twenty-three healthy women were recruited at the Samsung Medical Center (SMC), Seoul, South Korea, between October 2021 and November 2022. Whole blood was extracted after obtaining informed consent from the participants with the approval of the SMC Institutional Review Board (IRB No. SMC 2019-08-119, SMC 2021-08-063).

Consent for publication

All the authors have read the manuscript and agreed to submit the paper to the journal.

Competing interests

The authors declare no competing interests.

Author details

¹Department of Health Sciences and Technology, SAHST, Sungkyunkwan University, Seoul, South Korea. ²Laboratory of Molecular Pathology and Theranostics, Samsung Medical Center, Sungkyunkwan University School of Medicine, Irwon-Ro 81, Gangnam-Go, Seoul 06351, South Korea. ³College of Pharmacy, Duksung Women's University, Seoul, South Korea. ⁴Department of Medicine, Division of Hematology-Oncology, Samsung Medical Center, Sungkyunkwan University School of Medicine, Seoul, South Korea. ⁵Department of Pathology and Translational Genomics, Samsung Medical Center, Sungkyunkwan University School of Medicine, Irwon-Ro 81, Gangnam-Go, Seoul 06351, South Korea.

Received: 9 April 2024 Accepted: 30 July 2024

Published online: 29 August 2024

References

- Ni HM, Williams JA, Ding WX. Mitochondrial dynamics and mitochondrial quality control. *Redox Biol.* 2015;4:6–13.
- Stehling O, Lill R. The role of mitochondria in cellular iron-sulfur protein biogenesis: mechanisms, connected processes, and diseases. *Cold Spring Harb Perspect Biol.* 2013;5(8):a011312.
- Zhao RZ, Jiang S, Zhang L, Yu ZB. Mitochondrial electron transport chain, ROS generation and uncoupling (Review). *Int J Mol Med.* 2019;44(1):3–15.
- Deshpande OA, Mohiuddin SS. *Biochemistry, Oxidative Phosphorylation.* Treasure Island (FL): StatPearls; 2024.
- Boyman L, Karbowski M, Lederer WJ. Regulation of Mitochondrial ATP Production: Ca(2+) Signaling and Quality Control. *Trends Mol Med.* 2020;26(1):21–39.
- Nath S. Integration of demand and supply sides in the ATP energy economics of cells. *Biophys Chem.* 2019;252:106208.
- Warburg O. On respiratory impairment in cancer cells. *Science.* 1956;124(3215):269–70.
- Gaude E, Frezza C. Tissue-specific and convergent metabolic transformation of cancer correlates with metastatic potential and patient survival. *Nat Commun.* 2016;7:13041.
- Viale A, Pettazzoni P, Lyssiotis CA, Ying H, Sanchez N, Marchesini M, et al. Oncogene ablation-resistant pancreatic cancer cells depend on mitochondrial function. *Nature.* 2014;514(7524):628–32.
- Hensley CT, Faubert B, Yuan Q, Lev-Cohain N, Jin E, Kim J, et al. Metabolic Heterogeneity in Human Lung Tumors. *Cell.* 2016;164(4):681–94.
- Davidson SM, Papagiannakopoulos T, Olenchok BA, Heyman JE, Keibler MA, Luengo A, et al. Environment Impacts the Metabolic Dependencies of Ras-Driven Non-Small Cell Lung Cancer. *Cell Metab.* 2016;23(3):517–28.
- Plitzko B, Loesgen S. Measurement of Oxygen Consumption Rate (OCR) and Extracellular Acidification Rate (ECAR) in Culture Cells for Assessment of the Energy Metabolism. *Bio Protoc.* 2018;8(10):e2850.
- Lark DS, Torres MJ, Lin CT, Ryan TE, Anderson EJ, Neuffer PD. Direct real-time quantification of mitochondrial oxidative phosphorylation efficiency in permeabilized skeletal muscle myofibers. *Am J Physiol Cell Physiol.* 2016;311(2):C239–45.
- Cheng H, Munro D, Pamerter ME. Dynamic calculation of ATP/O ratios measured using Magnesium Green (MgGr). *MethodsX.* 2021;8:101520.
- Preble JM, Pacak CA, Kondo H, MacKay AA, Cowan DB, McCully JD. Rapid isolation and purification of mitochondria for transplantation by tissue dissociation and differential filtration. *J Vis Exp.* 2014;91:e51682.
- Divakaruni AS, Wiley SE, Rogers GW, Andreyev AY, Petrosyan S, Lovisach M, et al. Thiazolidinediones are acute, specific inhibitors of the mitochondrial pyruvate carrier. *Proc Natl Acad Sci U S A.* 2013;110(14):5422–7.
- Marcussen M, Larsen PJ. Cell cycle-dependent regulation of cellular ATP concentration, and depolymerization of the interphase microtubular network induced by elevated cellular ATP concentration in whole fibroblasts. *Cell Motil Cytoskeleton.* 1996;35(2):94–9.
- Farhadi P, Yarani R, Valipour E, Kiani S, Hoseinkhani Z, Mansouri K. Cell line-directed breast cancer research based on glucose metabolism status. *Biomed Pharmacother.* 2022;146:112526.
- Boengler K, Kosiol M, Mayr M, Schulz R, Rohrbach S. Mitochondria and ageing: role in heart, skeletal muscle and adipose tissue. *J Cachexia Sarcopenia Muscle.* 2017;8(3):349–69.
- Langen P, Hucho F. Karl Lohmann and the discovery of ATP. *Angew Chem Int Ed Engl.* 2008;47(10):1824–7.
- Sun L, Zhang L, Chen J, Li C, Sun H, Wang J, et al. Activation of Tyrosine Metabolism in CD13+ Cancer Stem Cells Drives Relapse in Hepatocellular Carcinoma. *Cancer Res Treat.* 2020;52(2):604–21.
- Gatt AP, Duncan OF, Attems J, Francis PT, Ballard CG, Bateman JM. Dementia in Parkinson's disease is associated with enhanced mitochondrial complex I deficiency. *Mov Disord.* 2016;31(3):352–9.
- Kurelac I, MacKay A, Lambros MB, Di Cesare E, Cenacchi G, Ceccarelli C, et al. Somatic complex I disruptive mitochondrial DNA mutations are modifiers of tumorigenesis that correlate with low genomic instability in pituitary adenomas. *Hum Mol Genet.* 2013;22(2):226–38.
- Astuti D, Latif F, Dallol A, Dahia PL, Douglas F, George E, et al. Gene mutations in the succinate dehydrogenase subunit SDHB cause susceptibility to familial pheochromocytoma and to familial paraganglioma. *Am J Hum Genet.* 2001;69(1):49–54.

25. Bandara AB, Drake JC, Brown DA. Complex II subunit SDHD is critical for cell growth and metabolism, which can be partially restored with a synthetic ubiquinone analog. *BMC Mol Cell Biol.* 2021;22(1):35.
26. Muller B, Lewis N, Adeniyi T, Leese HJ, Brison DR, Sturmey RG. Application of extracellular flux analysis for determining mitochondrial function in mammalian oocytes and early embryos. *Sci Rep.* 2019;9(1):16778.
27. Shin JS, Kim TG, Kim YH, Eom SY, Park SH, Lee DH, et al. Senescent tumor cells in colorectal cancer are characterized by elevated enzymatic activity of complexes 1 and 2 in oxidative phosphorylation. *J Pathol Transl Med.* 2023;57(6):305–14.
28. Divakaruni AS, Rogers GW, Murphy AN. Measuring Mitochondrial Function in Permeabilized Cells Using the Seahorse XF Analyzer or a Clark-Type Oxygen Electrode. *Curr Protoc Toxicol.* 2014;60(25 2):1–16.
29. Hinkle PC. P/O ratios of mitochondrial oxidative phosphorylation. *Biochim Biophys Acta.* 2005;1706(1–2):1–11.
30. Siegel MP, Wilbur T, Mathis M, Shankland EG, Trieu A, Harper ME, et al. Impaired adaptability of in vivo mitochondrial energetics to acute oxidative insult in aged skeletal muscle. *Mech Ageing Dev.* 2012;133(9–10):620–8.
31. Seyfried TN, Arismendi-Morillo G, Mukherjee P, Chinopoulos C. On the Origin of ATP Synthesis in Cancer. *iScience.* 2020;23(11):101761.
32. Szostaczuk N, van Schothorst EM, Sanchez J, Priego T, Palou M, Bekkenkamp-Grovenstein M, et al. Identification of blood cell transcriptome-based biomarkers in adulthood predictive of increased risk to develop metabolic disorders using early life intervention rat models. *FASEB J.* 2020;34(7):9003–17.
33. Tomas C, Brown A, Strassheim V, Elson JL, Newton J, Manning P. Cellular bioenergetics is impaired in patients with chronic fatigue syndrome. *PLoS ONE.* 2017;12(10):e0186802.
34. Hartman ML, Shirihai OS, Holbrook M, Xu G, Kocherla M, Shah A, et al. Relation of mitochondrial oxygen consumption in peripheral blood mononuclear cells to vascular function in type 2 diabetes mellitus. *Vasc Med.* 2014;19(1):67–74.

Publisher's Note

Springer Nature remains neutral with regard to jurisdictional claims in published maps and institutional affiliations.